TDA Progress Report 42-92

October–December 1987

DSS 14 64-Meter Antenna S- and X-Band Efficiency and System Noise Temperature Calibrations, September 1987

S. D. Slobin
Radio Frequency and Microwave Subsystems Section

This article is the third in a series documenting the efficiency and noise temperature characteristics of the DSN 64-meter antenna network prior to its upgrading to 70-meter configuration. DSS 14 (Goldstone, California) is the last of the three large antennas to be upgraded, and the test results presented here document its performance just prior to its downtime during the end of 1987. Antenna area efficiency was found to be somewhat higher at DSS 14 than at DSS 43 (Australia) and DSS 63 (Spain). The peak X-band efficiency was determined to be 49.8 percent (without atmosphere), compared with 45.4 percent and 45.1 percent for DSS 43 and DSS 63, respectively. The X-band zenith system noise temperature was found to be 1 to 3 kelvins higher than at the other two stations, depending on which maser was chosen for the measurements. Ascribing efficiency differences to small-scale antenna surface roughness, DSS 14 may be regarded as having a 1.5- to 1.6-mm rms surface as compared to the other two antennas with 1.7- to 1.8-mm rms surfaces.

I. Introduction

This article is the third in a series documenting the performance of the DSN 64-meter network prior to its upgrading to 70-meter configuration. DSS 14 is the third of the three large antennas to be modified; DSS 63 was upgraded in May 1987, and DSS 43 in September 1987. DSS 14 will achieve its final configuration by early 1988. The S- and X-band performance of the overseas 64-meter antennas is documented in [1] and [2].

Antenna calibration measurements were taken during the months of August and September 1987. Because of a change in radiometer calibration technique in the middle of the calibration project (hourly noise diode calibration instead of approximately once every 6 hours), only those data from days 258, 267, and 270 were used in the final data reduction. The radio sources used on those days as standard efficiency calibrators were 3C123, 3C274, and 3C286. Subsequent to the DSS 14 tests, modifications were made in the DSN radio source list[1] which affected these sources. The changes involved both flux and source size corrections, and it was necessary to

[1] M. Klein, A. Freiley, and P. Richter, *DSN Radio Source List for Antenna Calibration*, JPL Report D-3801, Rev. B (internal document), Jet Propulsion Laboratory, Pasadena, California.

apply these corrections to the measured efficiency values after the fact. Since 3C274 is one of the strongest DSN calibrators visible from both the northern and southern hemispheres (and is also used in both the DSS 43 and DSS 63 calibrations), it must be accepted that the efficiency calibrations based on this source, as published in [1] and [2], are slightly in error. The source size correction for 3C274 increased 0.369 percent. This would have the effect of increasing the apparent antenna efficiency by approximately half this amount (for a 50 percent efficient antenna). The effect of these changes on the published DSS 43 and DSS 63 performance values will be discussed later.

The DSS 63 calibration article [1] contains a great amount of detail regarding calibration methods used and techniques involved in data reduction and analysis. That reference should be used if any uncertainty of meaning arises in the reading of this article.

Data taken on the three listed days appear to be generally well-behaved, and the weather was noted as clear with wind not exceeding 15 mph. Psychrometric data were taken hourly during the measurements, and this proved to be extremely useful in determining adjustments for the "no-atmosphere" antenna calibration values. Based on the temperature and relative humidity values given in the calibration report, an average weather model for DSS 14 was developed for the 13-day span of measurements. Total atmospheric attenuation was determined to be surprisingly constant over this time period, even though the temperature and relative humidity values varied greatly (e.g., the temperature ranged from 58°F to 103°F, and the relative humidity varied, almost inversely, from 89 percent down to 7 percent). For the purposes of this article, the S-band zenith attenuation was determined to be 0.025 dB, and the X-band zenith attenuation was determined to be 0.033 dB. These may be contrasted with the DSS 43/63 model of 0.03 dB and 0.04 dB, respectively, for S- and X-band, for year-average attenuation at those temperate locales.

After the data were corrected for flux and source size as given in [3], it became clear that the efficiency values determined using 3C123 were about 3 percent high (about 1-1/2 efficiency percent) when compared to the efficiency values determined using sources 3C274 and 3C286. This difference was the same at S- and X-bands, and did not seem to be a function of elevation angle (which would rule out a weather model error for data taken on different days). After consultation (M. J. Klein, private communication), it was decided to adjust the S- and X-band efficiency values by the factor 0.97 for those antenna efficiencies determined using radio source calibrator 3C123. This radio source calibrator is about one-fourth as strong as the strongest DSN standard calibrator (3C274), and since 3C274 and 3C286 give results agreeing very well with one another, 3C123 efficiency determinations were changed. It is possible that 3C123 flux has changed; however, at this time, the source of the discrepancy has not been determined. The problem will be examined in the future, and 3C274/3C123 comparisons using other antennas at Goldstone may help resolve it. Although both 3C274 and 3C123 were used in the DSS 63 calibration [1], the 3 percent difference was not apparent in those data.

II. Antenna Area Efficiency

Figures 1 and 2 show the S-band antenna area efficiencies both with and without the atmospheric attenuation included. Note that area efficiency is referenced to a uniformly illuminated aperture, 64 meters in diameter, at the given frequencies. For S-band (2295 MHz), the 100 percent efficient antenna gain is 63.75 dBi; for X-band (8420 MHz) it is 75.04 dBi.

It should be noted that data taken at the low elevation angles (less than 10 degrees) show much scatter. This is possibly due to atmospheric attenuation changes from point to point or scintillations that affect the noise temperature measurement in the on-source position. Also shown in the figures are second-order curve fits to the data. Note that the curve fit in Fig. 2 (S-band efficiency without atmosphere) actually curves slightly upward! This is obviously a curve-fitting anomaly, with a possible contribution from a slight atmospheric model error. It would seem reasonable to assume that the S-band efficiency is nearly a constant 59.4 percent at all elevation angles. The data do not warrant a more complex description.

Figures 3 and 4 show the X-band area efficiencies both with and without atmosphere. Note again the extreme spread of measured values at elevation angles below 30 degrees. This undoubtedly contributes to the large uncertainties in the shape of the curve, even though the tight clustering of points in the 40- to 70-degree elevation region appears to determine the peak value fairly well.

Table 1 gives the coefficients of the second-order curve fits in Figs. 1 through 4. Also given in the table are peak values of efficiency and the elevation angles at which they occur.

III. System Noise Temperature

Figures 5 and 6 show the S-band system noise temperature both with and without atmospheric contribution. The two sets of data represent data taken with two different masers. The upper curve shows data taken with the Block V maser; the lower curve is that taken with the SPD maser in a low noise path. Because of the limited elevation angle range of the lower data set, it was not curve-fitted to represent system noise tem-

perature as a function of elevation angle. The upper data set in Figs. 5 and 6 was fitted with a fourth-order curve, the coefficients of which are given in Table 2. Note that in Fig. 5 (above 65 degrees) and in Fig. 6 (above 70 degrees) the extrapolated values of the curve fit are created to be constant, as the actual fourth-order curve varies radically from what would be considered a reasonable extrapolation.

Figures 7 and 8 present the X-band system noise temperatures both with and without atmospheric contribution. Note again two sets of data. The upper data set was taken with the TWM-1 maser, while the lower data set was taken with the TWM-2 maser. Only the upper data set was curve-fitted, owing to the limited elevation angle range of the lower set. It appears that a constant difference (approximately 3 kelvins) separates the two sets. For the X-band curve fit in Fig. 7, the extrapolation is constant above 75 degrees; for Fig. 8 it is constant above 85 degrees.

IV. Error Analysis

A comprehensive review of error sources in this antenna calibration scheme is given in [1] and [2]. It bears repeating that the major contributor to the error in determination of antenna efficiency is the uncertainty regarding radio source flux density. It is estimated that this uncertainty at S-band is ±0.3 dB(3σ) (±3 percent, 1σ); at X-band it is ±0.5 dB (3σ) (±4 percent, 1σ). Indeed, the 3 percent efficiency adjustments at S- and X-band are perhaps indicative of this problem. The absolute accuracy in the determination of antenna efficiency for the DSS 14 antenna (as determined similarly for DSS 43 and DSS 63) is thus stated as:

S-band: ±0.4 dB (3σ)

X-band: ±0.6 dB (3σ)

V. Comparison of Measured and Expected Antenna Efficiencies

As described in [1] and [2], a comparison was made among the 64-m X-band antenna performance expectations as given by the physical optics (PO) and geometrical theory of diffraction (GTD) programs. The PO analysis was described in great detail in those references and will not be repeated here. Of interest here are the GTD calculations of antenna efficiency as a function of elevation angle, taking into account the long-period (~1 to 30 meters) gravitational deformation of the main reflector surface. The GTD-generated efficiency curve is modified by known or postulated hardware loss (0.821 dB; cf. Table 3, items 8–11 in [1]), and this curve is then further modified by various amounts of so-called Ruze loss, the loss of antenna efficiency due to small-scale (~1- to 100-centimeter) surface roughness.

Figure 9 shows the GTD curves with three levels of surface roughness: 1.06 mm (the design expectation of rms panel and subreflector tolerance), 1.5 mm, and 1.6 mm. It is seen that the DSS 14 antenna efficiency curve corresponds over the entire elevation angle range to an rms surface tolerance of 1.55 mm. Also shown on this curve are the DSS 43 and DSS 63 efficiencies, which, as stated in previous articles, correspond to surface tolerances of 1.7 to 1.8 mm. Note that the DSS 63 antenna differed structurally from the DSS 14 and DSS 43 antennas, and thus the greater efficiency falloff of that antenna is not surprising.

VI. Future Updates for DSS 14, 43, and 63 64-Meter Efficiencies

Due to a recent change in the source size correction factor for radio source 3C274 (see footnote 1), there exists a very small discrepancy in the efficiency values determined for DSS 14 as compared with those determined for DSS 43 and DSS 63. For example, it is possible that the 0.369 percent increase in X-band source size correction might increase the efficiencies of the overseas antennas by as much as 0.2 percent (e.g., from 50.0 percent to 50.2 percent). This increase is small compared to the scatter of data points (cf. Figs. 3 and 4 and Table 1), and thus may be judged as not significant in a statistical sense. Consultation with one of the authors of JPL Report D-3801 (see footnote 1) revealed that the present source size correction value should be considered interim only, and that an updated and highly improved document will be published within the next several months.[2] His advice in the matter of efficiency adjustment was to make no changes at this time. This article and its two precursors used radio source flux and size corrections which were the latest available at the time. Updated values of efficiency for the three stations can be computed when the future DSN radio source list becomes available, although values of tenths of an efficiency percent are not judged significant in view of the absolute accuracy levels presently attainable.

[2]M. J. Klein, private communication, Jet Propulsion Laboratory, Pasadena, California.

Acknowledgments

The author wishes to thank the engineers at the Goldstone DSCC, in particular Bill Wood and Tim Gregor, for their efforts in obtaining the data needed for this article. The M&I Group members Jim McCoy and Jerry Crook assisted with much-needed equipment maintenance.

References

[1] S. D. Slobin, "DSS-63 64-Meter S- and X-Band Efficiency and System Noise Temperature Calibrations," *TDA Progress Report 42-90*, vol. April–June 1987, Jet Propulsion Laboratory, Pasadena, California, pp. 103–115, August 15, 1987.

[2] S. D. Slobin, "DSS-43 64-Meter S- and X-Band Efficiency and System Noise Temperature Calibrations," *TDA Progress Report 42-90*, vol. April–June 1987, Jet Propulsion Laboratory, Pasadena, California, pp. 116–126, August 15, 1987.

Table 1. Coefficients of second order curve fits for antenna area efficiencies

efficiency = $a_0 + a_1\theta + a_2\theta^2$

where θ = elevation angle, degrees

Coefficient/parameter	S-band (2295 MHz)	X-band (8420 MHz)
	With atmosphere (cf. Fig. 1)	With atmosphere (cf. Fig. 3)
a_0	0.567571	0.434121
a_1	7.446475E-04	2.234165E-03
a_2	-5.887066E-06	-2.082133E-05
Peak efficiency, %	0.59112	0.49405
Peak angle, deg	63.244	53.651
Standard deviation, %	0.00354	0.00853
	Without atmosphere (cf. Fig. 2)	Without atmosphere (cf. Fig. 4)
a_0	0.592390	0.457946
a_1	1.936510E-06	1.572380E-03
a_2	4.675295E-07	-1.541394E-05
Peak efficiency, %	0.594 (see text	0.49805
Peak angle, deg	(see text)	51.005
Standard deviation, %	(see text)	0.00859

Table 2. Coefficients of fourth-order curve fits for S- and X-band system noise temperatures

$$T_{system} = a_0 + a_1\theta + a_2\theta^2 + a_3\theta^3 + a_4\theta^4$$

where θ = elevation angle, degrees

Coefficient/parameter	S-band (2295 MHz)[a]	X-band (8420 MHz)[b]
	With atmosphere (cf. Fig. 5)	With atmosphere (cf. Fig. 7)
a_0	4.919551E+01	5.836215E+01
a_1	-2.040157E+00	-2.234962E+00
a_2	6.445888E-02	6.128831E-02
a_3	-9.468854E-04	-7.517988E-04
a_4	5.169310E-06	3.378224E-06
	Note: If $\theta \geq 65$ deg, $T = 21.161$ K	Note: If $\theta \geq 75$ deg, $T = 25.211$ K
Zenith noise temperature, K	21.161	25.211
Standard deviation, K	0.334	0.358
	Without atmosphere (cf. Fig. 6)	Without atmosphere (cf. Fig. 8)
a_0	2.727111E+01	3.355993E+01
a_1	-2.675004E-01	-5.586415E-01
a_2	2.027795E-03	1.278769E-02
a_3	2.917834E-05	-1.356839E-04
a_4	-3.911682E-07	5.376014E-07
	Note: If $\theta \geq 70$ deg, $T = 19.098$ K	Note: If $\theta \geq 85$ deg, $T = 23.203$ K
Zenith noise temperature, K	19.098	23.203
Standard deviation, K	0.239	0.284

[a]S-band (2295 MHz) specs: Maser SPD Blk IV, S/N 4002, 1.83 K; Maser Blk V, S/N 5002, 4.48 K.

[b]X-band (8420 MHz) specs: Maser Blk II, TWM-2, S/N 2007, 3.46 K; Maser Blk IIA, TWM-1, S/N 2011, 3.82 K.

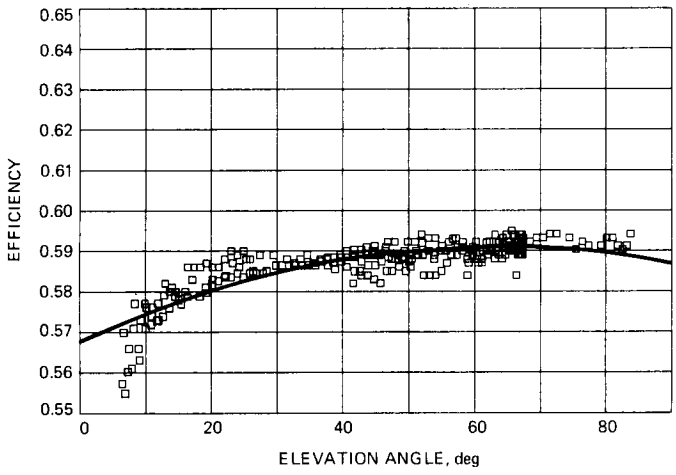

Fig. 1. DSS 14 64-m S-band (2295-MHz) area efficiency with atmospheric attenuation included

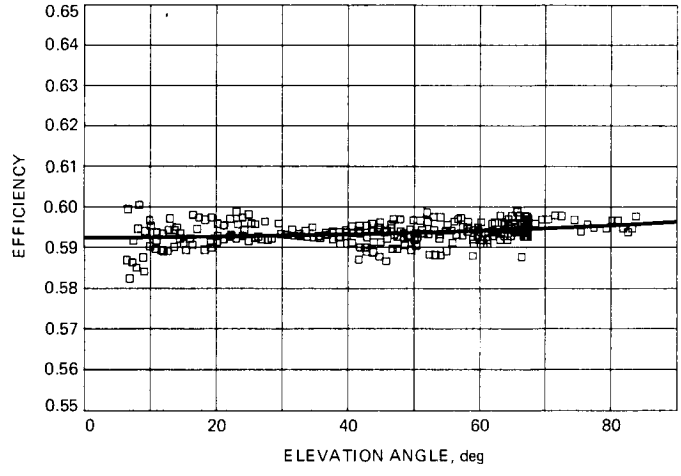

Fig. 2. DSS 14 64-m S-band (2295-MHz) area efficiency without atmospheric attenuation

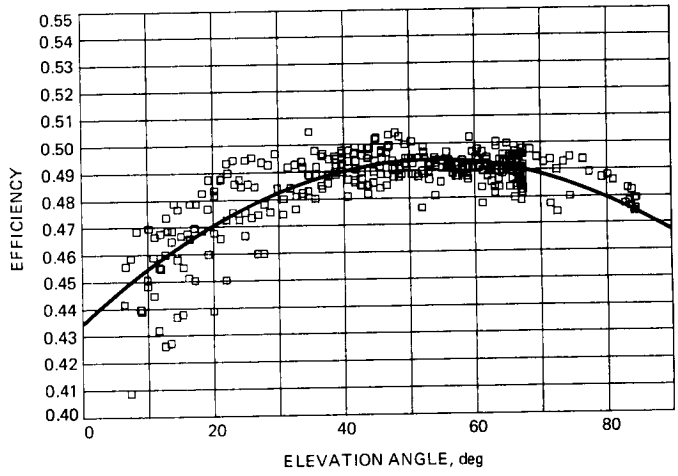

Fig. 3. DSS 14 64-m X-band (8420-MHz) area efficiency with atmospheric attenuation included

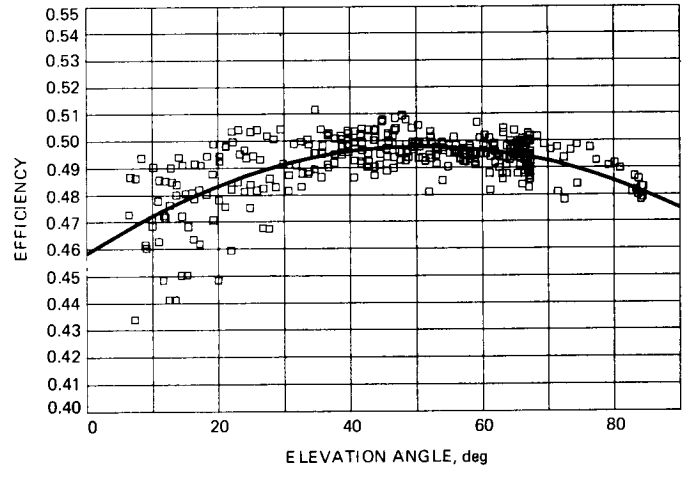

Fig. 4. DSS 14 64-m X-band (8420-MHz) area efficiency without atmospheric attenuation

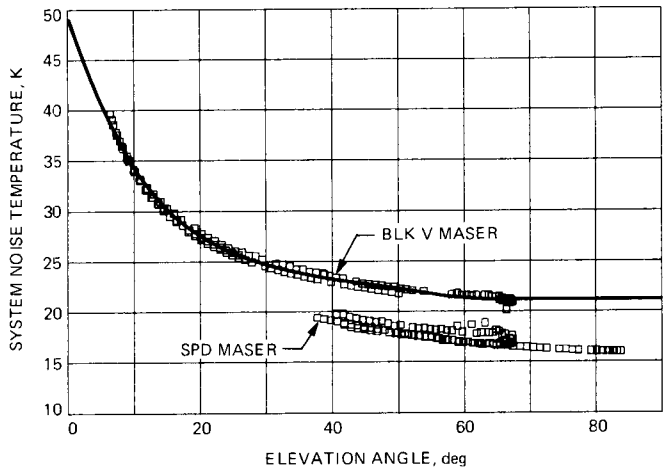

Fig. 5. DSS 14 64-m S-band (2295-MHz) system noise temperature, including atmospheric contribution

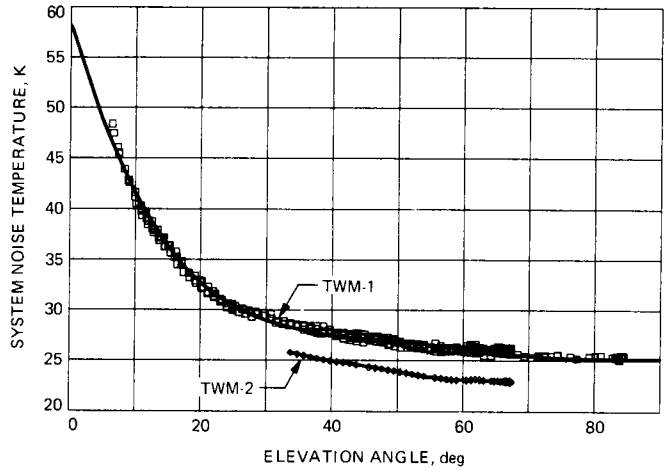

Fig. 7. DSS 14 64-m X-band (8420-MHz) system noise temperature, including atmospheric contribution

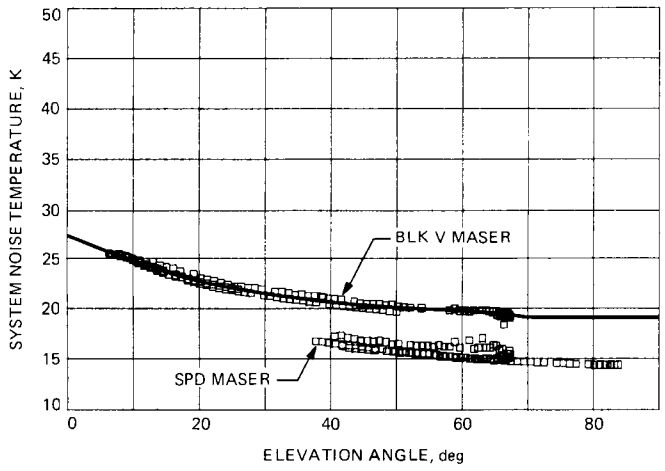

Fig. 6. DSS 14 64-m S-band (2295-MHz) system noise temperature without atmospheric contribution

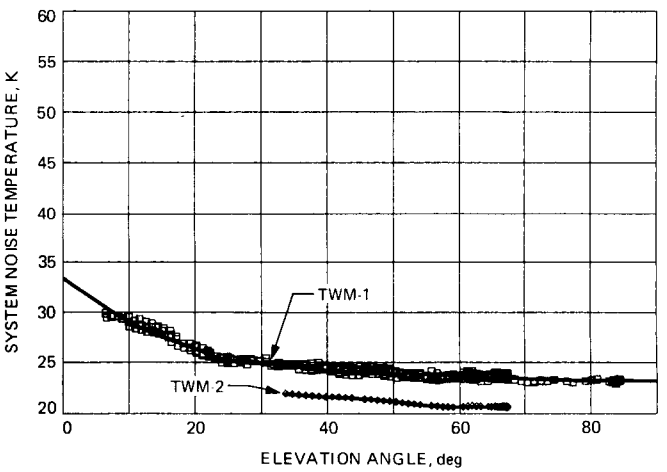

Fig. 8. DSS 14 64-m X-band (8420-MHz) system noise temperature without atmospheric contribution

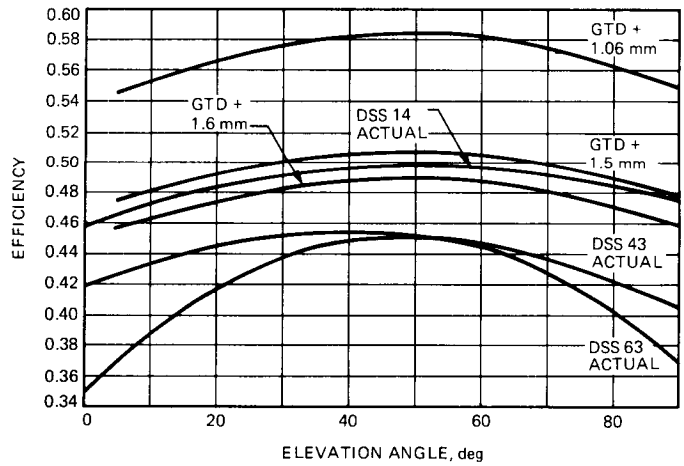

Fig. 9. Comparison of DSS 14, 43, and 63 64-m X-band measured efficiency and GTD-calculated efficiency for various Ruze surface tolerance values, without atmosphere